High-contrast transparency comb of the electromagnetically-induced-transparency memory

Sheng-Jun Yang,[1,2,3] Jun Rui,[1,2,3] Han-Ning Dai,[1,2,3] Xian-Min Jin,[1,2,4] Shuai Chen,[1,2,3,*] and Jian-Wei Pan[1,2,3,†]

[1]*Hefei National Laboratory for Physical Sciences at Microscale and Department of Modern Physics,*
University of Science and Technology of China, Hefei, Anhui 230026, China
[2]*CAS Center for Excellence and Synergetic Innovation Center in Quantum Information and Quantum Physics,*
University of Science and Technology of China, Hefei, Anhui 230026, China
[3]*CAS-Alibaba Quantum Computing Laboratory, Shanghai 201315, China*
[4]*State Key Laboratory of Advanced Optical Communication Systems and Networks, School of Physics and Astronomy,*
Shanghai Jiao Tong University, Shanghai 200240, China

Quantum interface of coherent optical field and atomic excitations plays an important role in quantum metrology and quantum information science. The electromagnetically-induced-transparency (EIT) technique has shown versatile and powerful capability in many applications during the last decades. By using efficient EIT-based memory, we directly observed single-photon-level Ramsey interference and also high-contrast spectral transparency comb with a visibility up to about 0.81 at around the resonant line in cold atoms. The interference fringes are mainly influenced by the pulse repetition period, the waveform overlap of the slowed and retrieved signal pulses, and the coherent lifetime of the EIT memory. All these factors have been investigated in detail. Such high-contrast interference fringe may offer us methods for precision measurement and potential applications in areas of atomic clock and magnetometry.

Coherent control and manipulation of atoms is becoming increasingly important in various quantum optics experiments. Discovery of the electromagnetically-induced-transparency (EIT) method [1], especially the ability of coherent slowing and storage of photons [2,3], has triggered tremendous exciting developments in quantum optics and quantum information science. Briefly, the quantum state of a weak signal pulse around an absorption line can be coherently mapped into and out of a stationary atomic state via a strong control field once the two-photon resonance condition is satisfied. Based on this, significant advances in areas of quantum memory and quantum information processing have been achieved in these years [4]. On the other hand, the EIT and coherent population trapping (CPT) techniques have also drawn worldwide attention in applications of atomic frequency standard [5,6], mainly due to their potential advantage in compact size design and high-frequency stability. For now, there have been various methods and proposals related to the EIT/CPT-based atom clock, from the Ramsey zone-separated interaction [7,8] to the Raman-Ramsey vapor cell approach [9,10], from the microwave cavity oscillation [11,12] to the all-optical coherent pulse scheme [13], from the two-pulse hyper-Ramsey method [14,15] and the double Lambda scheme [16,17] to the pulse-train coherence accumulation and comb transparency [18,19], etc. All efforts are towards a new generation of time keeping for various specific applications. However, though significant advances have been achieved, most of them have some kind of drawback, like annoying influence of light shift, cavity pulling, instability of

atomic population, and noninteracting background noise, all of which need great effort to harness.

In this paper, combining techniques of the EIT memory [2,3] and the time-domain Ramsey interference [20], we have obtained high-contrast spectral transparency comb of a signal field around the resonant transition in Rubidium cold atoms. The transparency comb is located on a zero-flat background, with an interference visibility up to 0.81. And the central transparency peak is much narrower compared with that of the ordinary EIT scheme. Such a high-contrast transparency comb may have potential applications where accurate and stable measurement of the atomic energy levels is needed. In contrast to the usual atomic frequency standards where Ramsey fringes are obtained by detecting population distribution of certain atomic states, we measure the interference fringes by photon counting of the signal pulses that are transparent through the atoms. The signal pulse is in the single-photon regime in our experiment. Thus, it has little influence or damage on the atom ensemble, and would dramatically reduce the preparation time of the atoms. What's more, the signal pulses are weak enough and have negligible ac-Stark shift. According to our experiment, the transparency comb is mainly determined by the pulse interval, the waveform overlap of the slowed and retrieved signal pulses, and the coherent lifetime of the collective atomic excitations. Elaborate parameter calibration could provide excellent signal-to-noise ratio of the transparency peaks. Yet there is no need of a microwave cavity or strict pulse width requirement to obtain the spectral fringes. Our experiment provides a novel scheme that may benefit the EIT-based atomic clock and frequency measurement.

The essence of our interference scheme lies on phase coherence of the EIT process. For a three-level Lambda-type
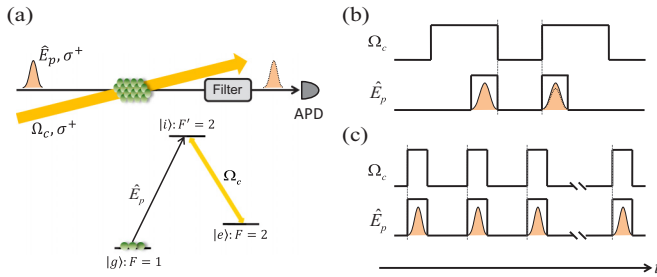
---

*shuai@ustc.edu.cn
†pan@ustc.edu.cn

(a)

(b)

(c)

FIG. 1. (a) Experiment scheme and energy structure of the ^{87}Rb atoms. All the atoms are initially in the ground state $|5S_{1/2}, F = 1\rangle$. The control (Ω_c) and signal ($\hat{\mathcal{E}}_p$) fields are right circularly polarized (σ^+), and resonant of the $D1$-line transition of $|F = 2\rangle \rightarrow |F' = 2\rangle$ and $|F = 1\rangle \rightarrow |F' = 2\rangle$, respectively. The transparent signal pulses are measured by a single-photon detector (APD), after passing through a Fabry-Perot cavity filter and an atomic filter successively. (b) Time sequence for the two-pulse EIT-Ramsey interference. Pulse width of the control field is 800 ns, and pulse width of the signal field is 300 ns. (c) Time sequence for the multipulse EIT-combed interference. Both the signal and control pulses are 200-ns width and are synchronously repeated hundreds of times after preparation of the atoms.

atomic system [inset in Fig. 1(a)], a strong control field Ω_c and a weak signal field $\hat{\mathcal{E}}_p$ are resonant of the atomic transition $|g\rangle \rightarrow |i\rangle$ and $|e\rangle \rightarrow |i\rangle$, respectively. There is no optical transition between the two ground states $|g\rangle$ and $|e\rangle$. And the atoms are initially prepared in the state $|g\rangle$. The strong control laser Ω_c could modulate the atomic dispersion and induce destructive interference between the two paths, that $|g\rangle - |i\rangle$ and $|g\rangle - |i\rangle - |e\rangle - |i\rangle$, for absorption of the weak signal field $\hat{\mathcal{E}}_p$. As a result, the signal field becomes transparent through the media, known as the electromagnetically induced transparency. In this process, the collective atom-photon state can be described as a dark-state polariton [21,22], that is a combination of the atomic spin-wave excitation $\hat{\sigma}_a$ and the optical signal field $\hat{\mathcal{E}}_p$,

$$\Psi(t) = \cos\theta\hat{\mathcal{E}}_p + \sqrt{N}\sin\theta\hat{\sigma}_a, \qquad (1)$$

where N is the total atom number, $\tan\theta = \sqrt{N}g/\Omega_c$, $g = \sqrt{\hbar\omega/2\epsilon_0 V}$ is single-photon Rabi frequency of the signal field, and Ω_c is Rabi frequency of the control field. When adiabatically decreasing laser power of the control field Ω_c, the coherent state of the signal field will be converted into the stationary atomic excitation $\hat{\sigma}_a$. Reversely, $\hat{\sigma}_a$ would be retrieved back to the original signal pulse if switching on the control field again. Thus, the quantum state can be successfully transferred between the flying photons and the stationary atoms. This is the basic mechanism of the EIT memory. Interfering the retrieved signal pulse with the subsequent incoming signal pulses, a time-domain Ramsey interference will be obtained [23]. Specifically, in our scheme, it is achieved by successive EIT-memory pulses, forming constructive and destructive interference between the slowed and retrieved signal pulses.

The experiments are carried out in a cold ^{87}Rb atom ensemble [Fig. 1(a)]. By 20 ms of the magneto-optical trapping (MOT), we prepare an atom ensemble with a temperature of
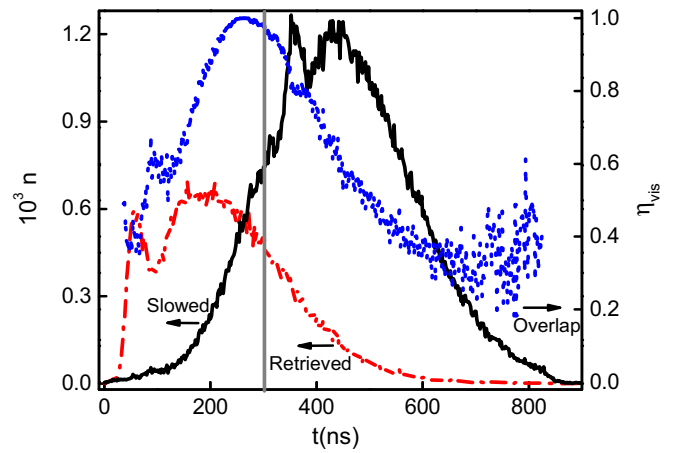

FIG. 2. Envelope of the slowed (black solid) and retrieved (red dashed) signal pulses, and the relative overlap parameter η_{vis} (blue dotted) between them. Pulse width of the incident signal field is 300 ns. Storage time of the retrieved signal pulse is 200 ns. Average of η_{vis} over the whole 800-ns duration is about 0.59.

$\sim 100\,\mu$K, and initially pump all the atoms into the ground state $|5S_{1/2}, F = 1\rangle$. Geomagnetic field and ambient stray magnetic field around the atoms have been compensated by three-axis Helmholtz coils. Optical depth of the atoms is about 22.6(1) on the $D1$-line transition of $|F = 1\rangle \rightarrow |F' = 2\rangle$. After each MOT loading, we carry out the EIT-based interference experiments for a duration of 3 ms. Two diode lasers (Toptica DL 100 at 795 nm), phase locked at a frequency of 6.835 GHz, provide the signal and control fields for the EIT memory. They are both right circularly polarized (σ^+), and propagate through the center of the atoms with an angle of $0.6°$. Beam widths of them are about 450 and $850\,\mu$m, respectively. The weak signal field is resonant or near resonant (detuning δ) of the $D1$-line transition of $|F = 1\rangle \rightarrow |F' = 2\rangle$, while the strong control field is resonant of $|F = 2\rangle \rightarrow |F' = 2\rangle$. The incident signal field is attenuated to about one photon in each pulse on average. Flying through the vacuum glass cell, the signal photons are measured by a single-photon detector after a Fabry-Perot cavity filter and an atomic filter successively.

First, we carry out the usual EIT memory. The incident signal field is 300-ns width and in the single-photon regime, which is about $3.8 \times 10^{-3}\,\mathrm{ns}^{-1}\mathrm{pulse}^{-1}$ without atomic absorption. Beam power of the control field is about $142\,\mu$W, with a fitting Rabi frequency Ω_c of 7.85(6) MHz. In Fig. 2, we show amplitude envelopes of the slowed signal pulse and the retrieved pulse after a storage time of 200 ns. Zero point of the x axis means switch-on of the control field. $n(t)$ in the left y axis is the measured photon counts per pulse for different detection instant t. The slowed time for the signal pulse is about 250 ns. Efficiency of the slowed light is about 47.1% at resonance corresponding to the original signal pulse. For the memory process, the control field is switched off at the 300-ns time instant and the slowed signal photon within the atom ensemble is converted into a stationary atomic excitation. The initial storage efficiency is about 24.4% and the coherent lifetime τ is about 2.8 μs. Clearly, the waveform of the retrieved signal pulse is similar to the slowed pulse between the time area of 300–800 ns shown in Fig. 2.

Now let's discuss the physical mechanism of the two-pulse EIT-Ramsey interference. In ideal conditions, coherence of the stored pulse is preserved during the memory. The key point for the interference is the wave package overlap between the slowed and retrieved signal pulses. In order to qualify the EIT-Ramsey interference, we define an overlap parameter η_{vis}, that similar to the usual interference visibility, as

$$\eta_{vis}(t) = 2\sqrt{n_s n_r}/(n_s + n_r), \qquad (2)$$

where $n_{s,r}$ is photon counts of the slowed and retrieved signal pulses at a time instant t and $\eta_{vis} \in [0, 1]$. Definition of η_{vis} is assumed that complete in-phase of the slowed and retrieved photons. Phase difference between them will induce the interference, and η_{vis} is the up-bound threshold of it. As shown in Fig. 2, η_{vis} is directly related to the waveform of the slowed and retrieved signal pulses, and the maximum is around the crossing point of them. The average of η_{vis} is about 0.59 over the whole 800-ns duration. The average value of η_{vis} is expected to be close to one by delicate modulation of the beam power and wave packet of the control and signal pulses [24,25].

For the two-pulse Ramsey interference, the time sequence is shown in Fig. 1(b). The control field initially maps a first signal pulse into the atoms. After a storage time of T, the control field is on again to convert the atomic excitations back to photons. Simultaneously another signal pulse is sent into the atoms. Back to Eq. (1), the atomic excitation $\hat{\sigma}_a$ is retrieved back to the signal field $\hat{\mathcal{E}}_{p,r}$ while phase preserving. The second slowed signal field is $\hat{\mathcal{E}}_{p,s}e^{-i\delta T}$, where δT is an accumulated phase difference due to the signal photon detuning δ. As a result, interference between these two pulses will produce a Ramsey fringe, that is $2|\hat{\mathcal{E}}_{p,r}\hat{\mathcal{E}}_{p,s}|\cos\delta T$.

In the Ramsey interference experiment, pulse widths of the signal and control fields are 300 ns and 800 ns, respectively. The control pulse is long enough to retrieve the whole stored signal photons. The duration of a two-pulse interference trial is 20 μs, and all the atoms are pumped back to the initial state $|F = 1\rangle$ at the end of each trial. Such operation is repeated for 150 times during the 3-ms memory duration. We record the signal photon number with tags of photon arriving time at the detector during the second control pulse. Resolution of our data acquisition system is 2 ns, enough for detailed analysis of the interference.

As shown in Fig. 3, we observe and analyze the EIT-Ramsey interference fringes by sweeping the signal photon detuning δ. Figures 3(a) and 3(b) are the Ramsey oscillation corresponding to the storage time T of 0.5 and 1.0 μs, respectively. Sum of the photon number is within the duration of 250–350 ns of the second signal pulse where η_{vis} is close to one as shown in Fig. 2. The y axis of $\mathcal{A}$ is normalized to the value of $2\sqrt{n_s n_r}$ where $\delta = 0$. The shallow gray envelope fitting with white line is equal to the oscillate amplitude of $\pm 2\sqrt{n_s n_r}$. The interference amplitudes of $\mathcal{A}(\delta)$ are equal to $n_{os} - (n_s + n_r)$, where n_{os} is the signal photon count within the 100-ns recording region. The positive and negative value of $\mathcal{A}$ represent constructive and destructive interference between the slowed and retrieved signal pulses. The maximum interference visibility of η_{vis}^{max} for the storage time of 0.5 and 1.0 μs are both about 0.71(1) at the resonance point. The
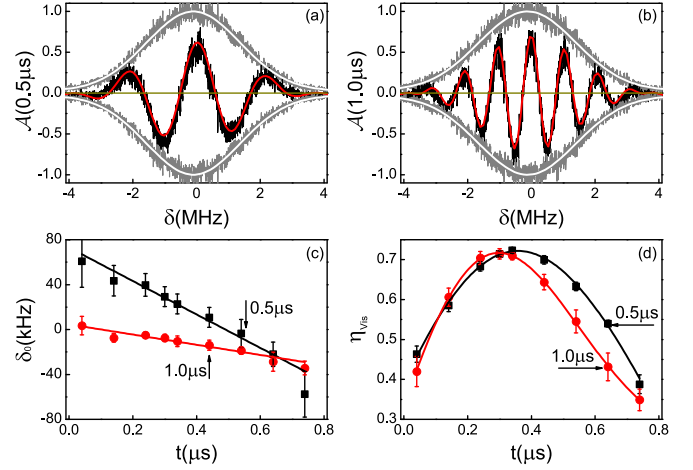

FIG. 3. The two-pulse EIT-Ramsey interference with a pulse separation of 0.5 and 1.0 μs. (a) and (b) The normalized interference amplitude $\mathcal{A}$ for different signal pulse detuning δ. Calculations are performed within a 100-ns duration around the crossing point of the slowed and retrieved pulses (Fig. 2). The dark black data (red line fitting) is the interference amplitude of the two signal pulses ($n_{s,r}$) while the shallow gray one (white line fitting) is the oscillation envelope of $\pm 2\sqrt{n_s n_r}$. Normalization of $\mathcal{A}$ is corresponding to the value of $2\sqrt{n_s n_r}$ where $\delta = 0$ MHz. (c) The central peak position δ_0 for a different counting interval of the signal photons, where duration of the photon count for each data is 100 ns. (d) The interference visibility η_{vis} of it. t in the x axis is the middle time instant of the analysis region.

deviation of η_{vis} from one is mainly due to spectral mismatching of the signal and control fields [26,27]. If including the whole signal pulse, we get the mean value of $\bar{\eta}_{vis} = 0.43(1)$ and 0.55(2) for $T = 0.5$ and 1.0 μs, respectively, which are a little smaller than the average overlap parameter of 0.59 in Fig. 2. We attribute it mainly to the decoherence of the atomic excitations during the memory. Higher value of $\bar{\eta}_{vis}$ at 1.0 μs is due to amplitude decrease of the retrieved signal pulse.

We also measure the central peak position and interference visibility for different region t of the second pulse, as shown in Figs. 3(c) and 3(d). Each data point is analyzed within a duration of 100 ns. The x axis is the middle time of the analysis region. In Fig. 3(c), detuning of the central peak drifts for a different analysis region of the pulse. It is due to the in-coincidence of the slowed and retrieved signal pulses and distortion of the group velocity [28,29]. Assuming $\varphi_0(t; \omega)$ as the additional phase shift for a different component of the signal pulse, we obtain the central frequency drift as

$$\delta_0(t) = -\frac{\varphi_0(t; \omega) - \varphi_0(t + t_{slow}; \omega)}{T - T_p} \simeq -\frac{\varphi_0^0 + \varphi_0^1 t}{T - T_p}, \quad (3)$$

where T_p is the signal pulse width, and the differential phase shift is linearly approximated as $\varphi_0^0 + \varphi_0^1 t$. The drift of the central frequency δ_0 is inversely proportional to the storage time T when $T_p \ll T$, and could be ignorable for a large value of T. The fitting slopes are 148(7) and 43(4) Hz/ns, respectively, for the storage time of 0.5 and 1.0 μs; the relative ratio between them is 3.3, close to the theoretical value of 3.5. In Fig. 3(d), we show the corresponding visibility η_{vis}
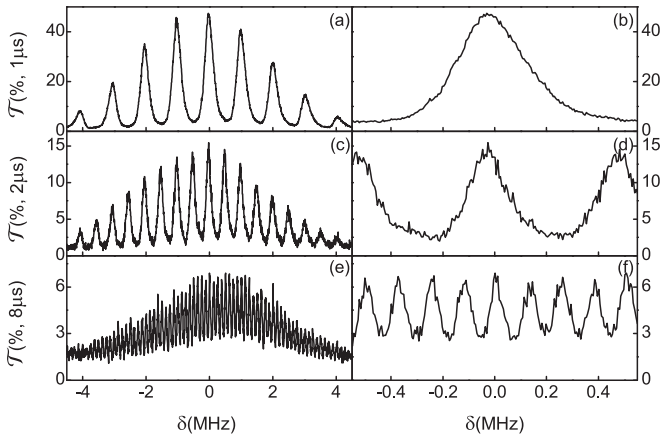
FIG. 4. The EIT-based transparency comb of the signal photons for a different pulse repetition period of $T = \{1, 2, 8\}\,\mu s$ from top to bottom. The x axis is detuning of the signal photons. The right subgraphs are enlargement of the central 1-MHz interval of the left. Photon counts are recorded over the whole signal pulse; the transparency rate $\mathcal{T}(\%)$ in the y axis is relative to a reference signal pulse without atoms.
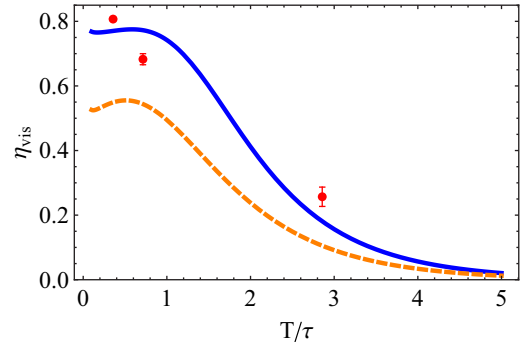

FIG. 5. The interference visibility η_{vis} of the EIT-combed transparency for different repetition period T. The red value of $\eta_{\text{vis}}(\delta \simeq 0\,\text{MHz}) = \{0.81(0), 0.68(2), 0.26(3)\}$ is related to the central peak shown in Fig. 4. Theoretical calculation of η_{vis} for the EIT-Ramsey (orange dashed) and EIT-combed (blue solid) schemes is also presented. The x axis is in units of the coherence lifetime $\tau \simeq 2.8\,\mu s$.

of the central interference peak. Obviously, the curve shape is consistent with the overlap parameter shown in Fig. 2.

In the EIT-Ramsey experiment, interference visibility is limited by the waveform mismatching between the slowed and retrieved signal pulses and different pulse width of the signal and control light. As we know, high-contrast interference is critically important in precision metrology. In the following, we use a multipulse sequence to generate a high-contrast transparency comb based on the EIT memory. The time sequence is shown in Fig. 1(c), where the repeated control and signal fields are exactly coincidental with each other and pulse width of them are 200 ns. The total pulse number is limited by the pulse repetition period and the 3-ms memory duration. The initial storage efficiency for a 200-ns signal pulse is about 37.9%. Pulse width of the slowed signal field is about 750 ns, longer than the incident pulse width. Thus, only part of the stored signal field is retrieved when the control field is switched on every time. The signal field that is not leaving the ensemble is converted into the atomic spin-wave excitation again when the control field is off. Thus, interference happens among the front of the slowed signal pulse ($\sim 3.6\%$) and all the retrieved components of the previous stored signal pulses (e.g., $\sim 10.1\%$ for the adjacent previous signal pulse). As coherence accumulation of these pulses would benefit the interference, higher visibility is expected.

In Fig. 4, we show the combed transparency structure of the signal photons for the pulse repetition period T of $\{1, 2, 8\}\,\mu s$ from top to bottom. Statistics of the signal photons is over the whole pulse area. Raw data is shown here without subtraction of the background noise. By varying the signal photon detuning, a comb-shaped transparency spectrum is observed and separation of the adjacent peaks is $1/T$. The value of the y axis is the transparency rate of $\mathcal{T}$ relative to the average photon number of an incident signal pulse without atoms. Diminution of the transparency rate and interference visibility for the long repetition period of T is due to the finite coherent lifetime τ. Interference visibility is about 0.81 at around

the central peak for $T = 1\,\mu s$. Compared with 0.55(2) of the previous EIT-Ramsey experiment, the multipulse scheme truly provides a better interference contrast.

Moreover, we calculate the transparency visibility of the other two-pulse repetition period at around the resonance and plot it in Fig. 5. The x axis is in units of the lifetime τ of the EIT memory. The visibility for $T = 2\,\mu s$ and $8\,\mu s$ are 0.68 and 0.26, respectively. Simultaneously, we also show the theoretical calculation for the EIT-Ramsey (orange dashed line) and EIT-combed (blue solid line) interference visibility, based on the experiment parameters. We measure the overlap parameter of the slowed and retrieved signal pulses when the incident signal pulse is 200-ns width, and get the average value $\bar{\eta}_{\text{vis}} \simeq 0.78$ as a threshold for calculation. Theoretically, interference visibility of the multipulse scheme is higher than that of the two-pulse scheme. As shown in Fig. 5, the experiment value is more or less consistent with the theoretical result.

As the coherent lifetime of the EIT memory in our experiment is about $2.8\,\mu s$, the full width at half maximum (FWHM) of the spectral peaks is limited to hundreds of kHz. The coherence lifetime can be further improved by decreasing the atomic temperature and choice of the magnetic insensitive transitions. For now, lifetime of the EIT memory has reached up to hundreds of milliseconds [30–32]. Resolution of the spectral transparency comb close to the sub-kHz scale is attainable. Besides in the experiment, we apply the single-photon-level pulses to identify quantum coherence and interference; for practical application, increasing laser power of the signal field while still satisfying the EIT condition will significantly improve the signal-to-noise ratio, and shorten time spent by the signal data accumulation. Moreover, the fringe visibility could be further improved by modulation of the wave package of the signal and control pulses [24,25]. For application of the EIT-based atom clock, we could apply a joint-period interference method, that is two-pulse Ramsey interference inside with a period T_1 and multirepeated for a longer period of $T_2 \neq \mathbb{N}T_1$, to avoid misuse of the adjacent peaks around the central one.

In conclusion, combining techniques of the EIT memory and the Ramsey interference, we have obtained a

high-contrast spectral transparency comb in the Rubidium cold atoms. Such high-interference contrast is reported for the first time compared with the other Ramsey experiments. Detailed physical mechanisms and various factors that influence the interference phase need further investigation. Our scheme may also be applied in other medias, like the vapor cell and the solid state. Our work may benefit applications in areas of the EIT-based atomic clock and magnetometry. We also wish it could offer a promising possibility to merge quantum memory and atom clock into a single setup, which is important in long-distance quantum communication and quantum repeaters.

[1] S. E. Harris, Phys. Today **50**, 36 (1997).

[2] M. D. Lukin, Rev. Mod. Phys. **75**, 457 (2003).

[3] M. Fleischhauer, A. Imamoglu, and J. P. Marangos, Rev. Mod. Phys. **77**, 633 (2005).

[4] L. Ma, O. Slattery, and X. Tang, J. Opt. **19**, 043001 (2017).

[5] J. Vanier, Appl. Phys. B **81**, 421 (2005).

[6] V. Shah and J. Kitching, Adv. At. Mol. Opt. Phys. **59**, 21 (2010).

[7] J. E. Thomas, P. R. Hemmer, S. Ezekiel, C. C. Leiby, R. H. Picard, and C. R. Willis, Phys. Rev. Lett. **48**, 867 (1982).

[8] P. R. Hemmer, M. S. Shahriar, H. Lamela-Rivera, S. P. Smith, B. E. Bernacki, and S. Ezekiel, J. Opt. Soc. Am. B **10**, 1326 (1993).

[9] G. Pati, K. Salit, R. Tripathi, and M. Shahriar, Opt. Commun. **281**, 4676 (2008).

[10] X. Liu, J.-M. Mérolla, S. Guérandel, C. Gorecki, E. de Clercq, and R. Boudot, Phys. Rev. A **87**, 013416 (2013).

[11] S. Micalizio, A. Godone, F. Levi, and C. Calosso, Phys. Rev. A **79**, 013403 (2009).

[12] B. Yan, Y. Ma, and Y. Wang, Phys. Rev. A **79**, 063820 (2009).

[13] T. Zanon-Willette, A. D. Ludlow, S. Blatt, M. M. Boyd, E. Arimondo, and J. Ye, Phys. Rev. Lett. **97**, 233001 (2006).

[14] V. I. Yudin, A. V. Taichenachev, C. W. Oates, Z. W. Barber, N. D. Lemke, A. D. Ludlow, U. Sterr, C. Lisdat, and F. Riehle, Phys. Rev. A **82**, 011804 (2010).

[15] N. Huntemann, B. Lipphardt, M. Okhapkin, C. Tamm, E. Peik, A. V. Taichenachev, and V. I. Yudin, Phys. Rev. Lett. **109**, 213002 (2012).

[16] T. Zanon, S. Guerandel, E. de Clercq, D. Holleville, N. Dimarcq, and A. Clairon, Phys. Rev. Lett. **94**, 193002 (2005).

[17] F.-X. Esnault, E. Blanshan, E. N. Ivanov, R. E. Scholten, J. Kitching, and E. A. Donley, Phys. Rev. A **88**, 042120 (2013).

[18] V. A. Sautenkov, Y. V. Rostovtsev, C. Y. Ye, G. R. Welch, O. Kocharovskaya, and M. O. Scully, Phys. Rev. A **71**, 063804 (2005).

[19] D. Hou, J. Wu, S. Zhang, Q. Ren, Z. Zhang, and J. Zhao, Appl. Phys. Lett. **104**, 111104 (2014).

[20] N. F. Ramsey, Rev. Mod. Phys. **62**, 541 (1990).

[21] M. Fleischhauer and M. D. Lukin, Phys. Rev. Lett. **84**, 5094 (2000).

[22] M. Fleischhauer and M. D. Lukin, Phys. Rev. A **65**, 022314 (2002).

[23] G. Campbell, M. Hosseini, B. M. Sparkes, P. K. Lam, and B. C. Buchler, New J. Phys. **14**, 033022 (2012).

[24] A. V. Gorshkov, A. André, M. Fleischhauer, A. S. Sørensen, and M. D. Lukin, Phys. Rev. Lett. **98**, 123601 (2007).

[25] I. Novikova, N. B. Phillips, and A. V. Gorshkov, Phys. Rev. A **78**, 021802 (2008).

[26] D. D. Yavuz, Phys. Rev. A **75**, 031801 (2007).

[27] G. Campbell, A. Ordog, and A. I. Lvovsky, New J. Phys. **11**, 103021 (2009).

[28] J. B. Khurgin, J. Opt. Soc. Am. B **22**, 1062 (2005).

[29] R. M. Camacho, M. V. Pack, and J. C. Howell, Phys. Rev. A **73**, 063812 (2006).

[30] U. Schnorrberger, J. D. Thompson, S. Trotzky, R. Pugatch, N. Davidson, S. Kuhr, and I. Bloch, Phys. Rev. Lett. **103**, 033003 (2009).

[31] Y. O. Dudin, R. Zhao, T. A. B. Kennedy, and A. Kuzmich, Phys. Rev. A **81**, 041805 (2010).

[32] S.-J. Yang, X.-J. Wang, X.-H. Bao, and J.-W. Pan, Nat. Photon. **10**, 381 (2016).